Proceedings of the ASME 2010 3rd Joint US-European Fluids Engineering Summer Meeting and 8th International Conference on Nanochannels, Microchannels, and Minichannels
FEDSM-ICNMM2010
August 1-5, 2010, Montreal, Canada

FEDSM-ICNMM2010-30891

VALIDATION OF LATTICE-BOLTZMANN AERODYNAMICS SIMULATION FOR VEHICLE LIFT PREDICTION

Bradley D. Duncan
Axel Fischer
Satheesh Kandasamy
Exa Corporation
Burlington, MA, USA

ABSTRACT

Simulation tools are used in the design of vehicles to reduce the cost of development and to find robust engineering solutions earlier in the design process. Prediction of drag using aerodynamics simulation is critical for assessing aerodynamic efficiency of designs, including upper body shape, underbody surfaces, wheels and aerodynamic treatments such as spoilers, deflectors and underbody covers. The Lattice-Boltzmann Simulation approach has been used broadly to simulate both steady and unsteady flow regimes accurately and to provide robust prediction of drag. Beyond drag, other vehicle performance metrics are now predicted using this type of simulation such as, for example, wind noise levels, heat exchanger performance, brake cooling and thermal protection of sensitive components. In particular, aerodynamic lift is important for production vehicles for assessing handling attributes at high speed.

In this paper, the validation of aerodynamics simulation for vehicle lift is examined and extended through a study of three detailed full-scale vehicles. For high-performance road vehicles the front- and rear-axle lift force, and the balance between them, are critical for driving dynamics for highway driving and must be considered along with the drag during development. Often a trade-off between lift and drag performance is required for a successful design. Furthermore, since the lift is highly dependent on the detailed pressure distribution in the underbody region and near the wheels, evaluation of lift should also account for on-road effects using rotating wheels and moving ground plane. In this study the drag, front lift and rear lift were evaluated using Lattice-Boltzmann Simulation and compared to full-scale wind-tunnel tests, using both static- and moving-ground configurations. Care was taken to include the effect of the floor boundary layer, suction system, moving belt and rotating tires, all of which are designed to emulate on-road conditions inside a wind-tunnel. The results show good prediction of both drag and lift performance, and provide confidence to extend the use of aerodynamic simulation for lift prediction earlier in the design process.

INTRODUCTION

Objectives

Lift performance is typically evaluated late in the design process by testing fully-detailed prototypes in a moving-ground wind-tunnel as well as on the road. At this late stage, changes to the design are costly and limited. For any vehicle

traveling at high speed, the handling of the vehicle is strongly driven by aerodynamics. The lift force on the front and rear of the vehicle, and the balance between the two is important for allowing the vehicle to respond to driver input as it also responds to the road and to the trajectory of motion. The design of the exterior shape of the vehicle determines the lift, including the smooth upper body surfaces, the design of the underbody, wheel openings, engine compartment inlets and outlets, and aerodynamic devices such as deflectors and spoilers. For motorsports applications it is common to use simulation tools for both lift and drag prediction and to evaluate performance of high-lift devices. However, for production vehicles, drag prediction is usually the focus of published validation studies, and much less validation data for lift is available. Simulation capability is needed, so that the overall shape of the vehicle can be design to achieve lift targets with minimal additional devices which may be costly as well as counter to design intent.

In this paper, validation data is presented for three vehicles tested in a moving-ground wind-tunnel facility to help assess the capability of simulation to predict front and rear lift. The wind tunnel type is open-jet with closed return. Three types of production vehicles were used, a sedan, a wagon, and a sports sedan. Detailed geometry was provided of the vehicle body, engine compartment and underbody, and also included detailed tire profiles scanned from the same tires used in the test. On the wagon, a rear underbody spoiler that significantly increases the rear lift was also removed to provide an additional test configuration, leading to a total of 4 configurations (sedan, wagon spoiler on, wagon spoiler off, sports sedan). The vehicles were tested at zero yaw angle and a speed of 140 kph, with a fixed ride height in the baseline (as delivered) configuration, as well as with taped front apertures. The sport sedan was tested with taped front only.

The objectives of this paper are to provide validation of lift prediction using aerodynamic simulation and to enable simulation to be used in advance of detailed prototype development in the design of upper body surfaces, underbody, and aerodynamic devices to meet vehicle handling targets.

Prediction of Lift in Simulation and Wind-Tunnels

Numerical simulation tools are in common use for prediction of aerodynamic lift and drag of vehicles of all types. The calculation of pressure distributions on rounded leading edges and smooth surfaces are straightforward in the absence of boundary layer separation. For less streamlined bodies, boundary layer separations are sure to occur, and can lead to strong gradients in the pressure distribution on the surface. At high enough speed, the flow in the boundary layer and separated regions becomes turbulent, and is dominated by more complex and fluctuating surface pressures. Aerodynamics simulations for lift of ground and aerospace vehicles rely on accurate solution methods that can solve the dynamics of realistic turbulent flow and resulting pressure distributions. For the upper surface of a fully-detailed automobile, this requires capturing the effect of small geometric details in the surface and the resulting effect on the local pressure distribution, boundary layer development and even separation. In the engine compartment, wheel and underbody regions, the pressure distribution is dominated by the losses in flow energy due to flow obstacles and impingements, and internal resistance in the grilles, ducts and radiator (and other porous media regions). The underbody flow region may have some smooth attached flow surfaces as well, in which the pressure distribution is determined by the flow velocity.

Physical testing for lift is complicated by the need for correct simulation of the on-road environment inside a test facility. Two examples of moving ground wind-tunnels are described in [1-3]. Accurate techniques for on-road measurements of lift are lacking, so wind-tunnel test facilities apply a variety of systems in order to minimize the effect of the stationary frame of reference. A belt system must be used to slide the floor at the same speed as the air in the test section. The boundary layer which builds on the static floor in front of the vehicle must be removed using a device such as a suction plate or tangential blowing slot, so that the moving belt can exert the correct amount of friction force on air above it, and on the vehicle and its wake. Finally, the wheels must be rotated to create the correct influence of the spinning surface on the surrounding pressure distribution and to create the right amount of flow through the wheel. It is well-understood that the systems needed to create the on-road environment in a wind-tunnel have their limitations, and their influence on the vehicle aerodynamics may not match the influence of the road on a moving vehicle. Nevertheless, moving-ground wind-tunnels are the state-of-the-art for measurement of lift of prototype and production vehicles. Proper consideration of the effects of the road-simulation systems in the wind-tunnel is necessary to use testing to design the vehicle.

In numerical simulation, the lift performance can be evaluated in an on-road test environment with negligible area blockage, idealized moving floor conditions, and uniform freestream conditions imposed very far from the vehicle. While this is the most useful testing mode for understanding the performance of the vehicle on the road, simulation can also be

used to bridge the gap between the on-road and moving-ground wind-tunnel environments, by including the effect of the ground simulation systems in the wind-tunnel. This is important for understanding these effects, as well as for building the needed confidence in simulation accuracy when validating simulation using wind-tunnel data.

APPROACH

Experiment

Four vehicle configurations were tested in a moving ground aerodynamics/aeroacoustics wind-tunnel:

- Production sedan
- Production wagon, underbody spoiler on
- Production wagon, underbody spoiler off
- Sport sedan

The first three vehicle configurations were tested with both open cooling apertures and taped front apertures (referred to as "no cooling" below). The vehicle is held at the required ride height by posts, and the wheels rest on large mini-belts which also rotate the wheels. The forces are transferred to the under-floor balance via both the posts and the wheel rotation units. The smooth steel center belt extends between the wheels and just forward and aft of the vehicle. The center belt is 5.5 m long and 1.0 m wide. A boundary layer suction system is used consisting of a larger primary suction plate at the wind-tunnel nozzle and a smaller secondary suction plate immediately in front of the belt.

Data was collected in a sequence of wind-tunnel floor modes:

- **Static, or fixed floor, mode**: this is similar to testing in other wind-tunnels with fixed ground, and does not employ any boundary layer control. The boundary layer thickness in this mode is 50mm at the inlet into the test section.
- **Boundary layer suction (BLS) mode**: in this mode the two boundary layer suction plates are activated to reduce the boundary layer thickness in front of the vehicle.
- **Center belt + BLS mode**: in this mode the center belt is activated under the vehicle in conjunction with the center belt.
- **Front wheels rotating or rear wheels rotating**: in this mode, the wheels are rotated by means of the minibelts. The front or rear wheels were rotated separately to see the individual effects.
- **Moving-ground mode**: this is the typical mode for simulating the on-road condition, and includes BLS, center belt, and rotating of front and rear wheels.

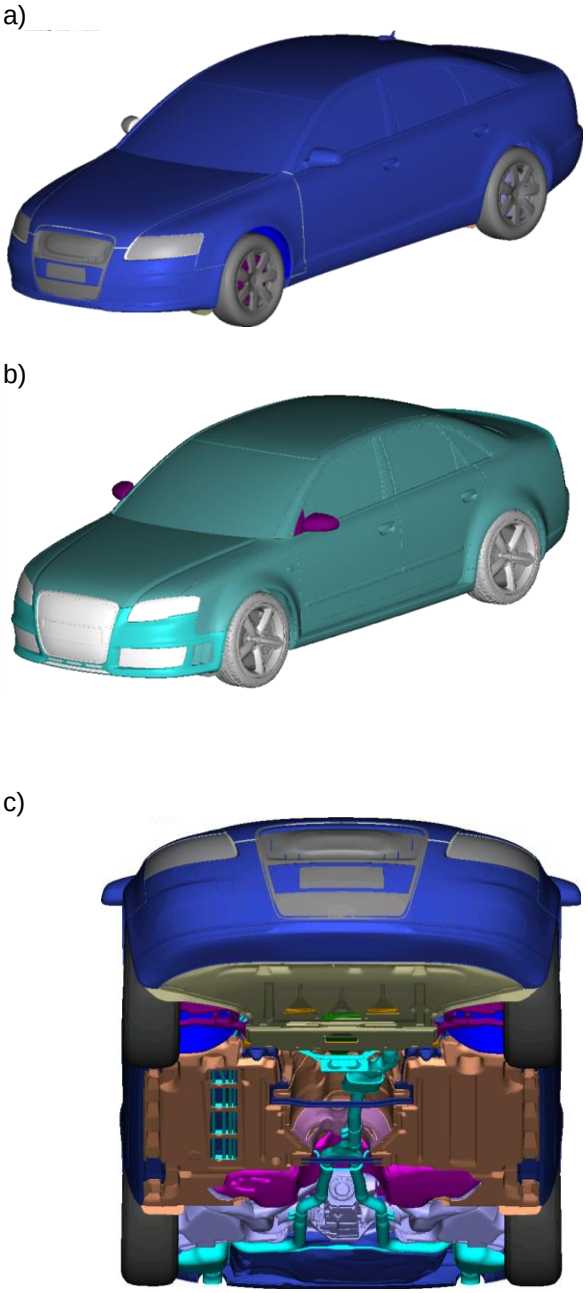

Figure 1. Vehicle configurations, a) sedan with taped front apertures, b) sport sedan with taped front apertures, c) underbody geometry for sedan

Simulation Setup

Numerical simulations were performed using the commercial software Exa PowerFLOW, which utilizes the Lattice-Boltzmann Method (LBM) approach to solve the transient, turbulent flow of air around the vehicle as represented by fully-detailed surface geometry. Examples of published validation studies using this simulation approach are in [4-14]. Selected data points from the wind-tunnel test were used for comparison with simulation for all four vehicle configurations (sedan, wagon spoiler on, wagon spoiler off, sports sedan), as shown in Figure 1. Some combinations were tested for open and closed front apertures and for four modes of the wind-tunnel floor (static, boundary layer suction, center belt + BLS, and moving-ground modes). The floor geometry is shown in Figure 2. In the simulation, boundary conditions on the floor were used to provide the boundary layer development in front of the test section to the specified boundary layer thickness, the effect of the primary and secondary suction plates, and the effect of the motion of the center belt and minibelts driving the wheels. The empty wind-tunnel floor model was simulated to test these boundary conditions and to compare to the experimental boundary layer thickness and floor pressure measurements. The wheel rotation was simulated using a "sliding wall" boundary condition on the entire tire and wheel, in which the surface is prescribed a rotational velocity. To show the influence of the wind-tunnel floor conditions the simulations were repeated in an on-road configuration with fully-moving ground and rotating wheels (but no suction system).

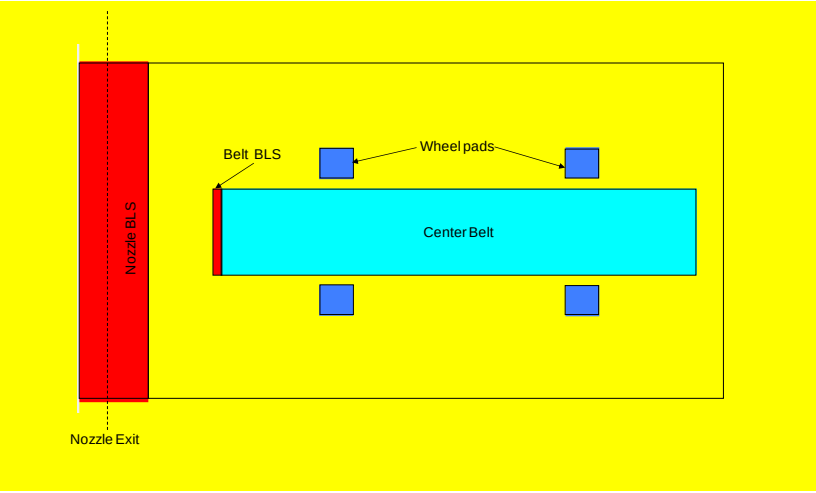

Figure 2. Schematic of wind-tunnel floor setup in simulation

Simulation of Empty Wind-Tunnel

Simulations were first performed using the wind-tunnel floor boundary conditions but with no vehicle present. Each of the wind-tunnel floor modes were tested. In addition a mode using only the primary suction plate was tested for comparison with experimental floor pressure data. The floor pressure is compared to measured floor pressures in Figure 3 and shows that the floor boundary condition captures the correct behavior of the suction system including the pressure level immediately in front of the vehicle (nose of the vehicle is at about -2.5m on the X axis).

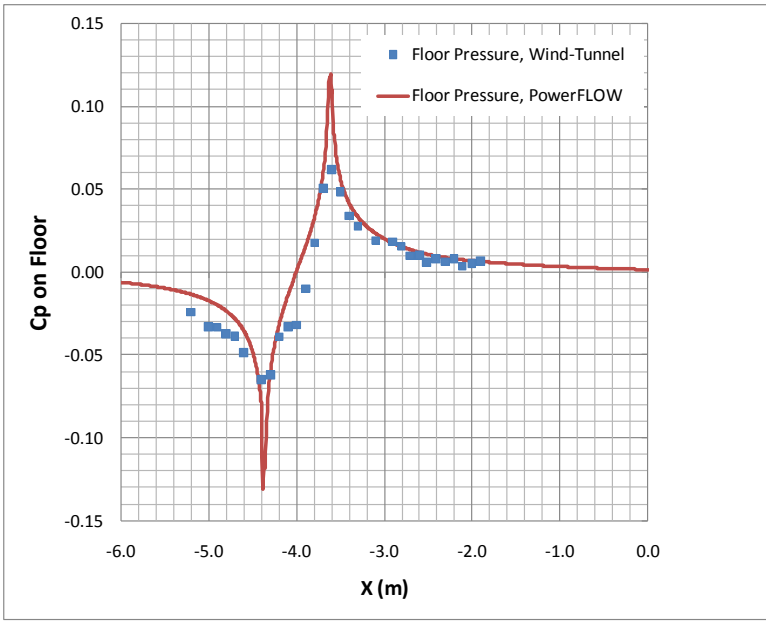

Figure 3. Pressure distribution on the floor, in a simulation of the tunnel floor (w/ no vehicle present) compared to experimental data. Only the primary suction is active for this comparison (no secondary suction).

RESULTS

Experimental Results

Effect of Vehicle Configuration. The experimental data is presented in Tables 1-5 and Figure 4. Tables 1-3 show data for the full set of wind-tunnel floor modes. Coefficient of drag (CD), front lift (CLF) and rear lift (CLR) are shown. To see the trends for the effect of floor mode, refer to Figure 4 which shows all data as deltas referenced to the Fixed Floor mode. The incremental data showing the effect of removing the underbody spoiler is shown in Table 4, and shows some small dependence on the floor mode. In general removing the spoiler increased drag in the open cooling configuration by ΔCD=+0.001 to +0.010 depending on the floor mode, and either decreased or increased drag in the no cooling configuration. The spoiler effect on lift was mainly felt on the rear, reducing the rear lift by ΔCLR=-0.053 to -0.089. The two data points for the sport sedan with no cooling are shown in Table 5, and the delta for moving ground vs. fixed floor is included in Figure 4.

Effect of Wind-Tunnel Floor Mode. The drag effect of activating the wind-tunnel floor systems includes some increase in drag due to boundary layer suction ΔCD=+0.008 to +0.011. Activating the center belt further increases the drag up to ΔCD=+0.005. Wheel rotation in turn reduces the drag in most cases, and effect of moving ground relative to fixed floor mode is mixed, from ΔCD=-0.006 to ΔCD=+0.012.

The lift trends are larger in magnitude and show a reduction in both front and rear lift from each component of the wind-tunnel floor system. The boundary layer suction provides a neutral to small front lift reduction (up to ΔCLF=-0.005). The center belt reduces the front lift by up to ΔCLF=-0.006, and fully moving ground mode has an overall effect of ΔCLF=-0.017 to ΔCLF=-0.026 relative to fixed floor. The rear lift effect of boundary layer suction is ΔCLR=-0.009 to ΔCLR=-0.013. Adding the center belt reduces the rear lift for most configurations by up to ΔCLR=-0.028. Fully moving mode has an overall effect to reduce rear lift relative to fixed floor mode, by ΔCLR=-0.025 to ΔCLR=-0.065.

Sedan Data, Experiment	Cooling			No Cooling		
	CD	CLF	CLR	CD	CLF	CLR
Fixed floor mode, no boundary layer control	0.296	0.147	0.072	0.271	0.068	0.116
Boundary layer suction (BLS) only	0.305	0.148	0.059	0.280	0.066	0.104
BLS and center belt	0.307	0.143	0.050	0.282	0.060	0.099
BLS, belt, rotate front wheels only	0.310	0.132	0.053	0.279	0.055	0.109
BLS, belt, rotate rear wheels only	0.289	0.141	0.043	0.266	0.057	0.083
Moving ground mode (BLS, belt, rotate wheels)	0.293	0.127	0.039	0.265	0.051	0.096

Table 1. Experimental data for sedan, open and closed cooling, for different wind-tunnel floor conditions.

Wagon Baseline with Underbody Spoiler, Experiment	Cooling			No Cooling		
	CD	CLF	CLR	CD	CLF	CLR
Fixed floor mode, no boundary layer control	0.316	0.106	0.082	0.299	0.032	0.141
Boundary layer suction (BLS) only	0.324	0.101	0.073	0.307	0.029	0.127
BLS and center belt	0.328	0.096	0.053	0.307	0.023	0.099
BLS, belt, rotate front wheels only	0.328	0.085	0.051	0.305	0.012	0.113
BLS, belt, rotate rear wheels only	0.316	0.092	0.031	0.298	0.020	0.069
Moving ground mode (BLS, belt, rotate wheels)	0.318	0.081	0.022	0.293	0.009	0.083

Table 2. Experimental data for baseline wagon (with rear underbody spoiler not removed), open and closed cooling, for different wind-tunnel floor conditions.

Wagon with No Underbody Spoiler, Experiment	Cooling			No Cooling		
	CD	CLF	CLR	CD	CLF	CLR
Fixed floor mode, no boundary layer control	0.317	0.105	0.015	0.293	0.030	0.052
Boundary layer suction (BLS) only	0.326	0.102	0.002	0.304	0.028	0.041
BLS and center belt	0.330	0.097	-0.005	0.308	0.023	0.046
BLS, belt, rotate front wheels only	0.334	0.083	-0.016	0.304	0.010	0.044
BLS, belt, rotate rear wheels only	0.323	0.089	-0.043	0.301	0.016	0.003
Moving ground mode (BLS, belt, rotate wheels)	0.328	0.079	-0.050	0.297	0.006	0.007

Table 3. Experimental data for wagon with rear underbody spoiler removed, open and closed cooling, for different wind-tunnel floor conditions.

Incremental Data for Removing Spoiler, Wagon, No Spoiler Minus Baseline	Cooling			No Cooling		
	ΔCD	ΔCLF	ΔCLR	ΔCD	ΔCLF	ΔCLR
Fixed floor mode, no boundary layer control	0.001	-0.001	-0.067	-0.006	-0.002	-0.089
Boundary layer suction (BLS) only	0.002	0.001	-0.071	-0.003	-0.001	-0.086
BLS and center belt	0.002	0.001	-0.058	0.001	0.000	-0.053
BLS, belt, rotate front wheels only	0.006	-0.002	-0.067	-0.001	-0.002	-0.069
BLS, belt, rotate rear wheels only	0.007	-0.003	-0.074	0.003	-0.004	-0.066
Moving ground mode (BLS, belt, rotate wheels)	0.010	-0.002	-0.072	0.004	-0.003	-0.076

Table 4. Experimental incremental data for wagon, baseline vs. rear underbody spoiler removed, for open and closed cooling, for different wind-tunnel floor conditions.

Sport Sedan Data, Experiment	Cooling			No Cooling		
	CD	CLF	CLR	CD	CLF	CLR
Fixed floor mode, no boundary layer control	--	--	--	0.277	0.013	0.122
Moving ground mode (BLS, belt, rotate wheels)	--	--	--	0.276	-0.004	0.097

Table 5. Experimental data for sport sedan, only closed cooling, with fixed and moving ground wind-tunnel floor

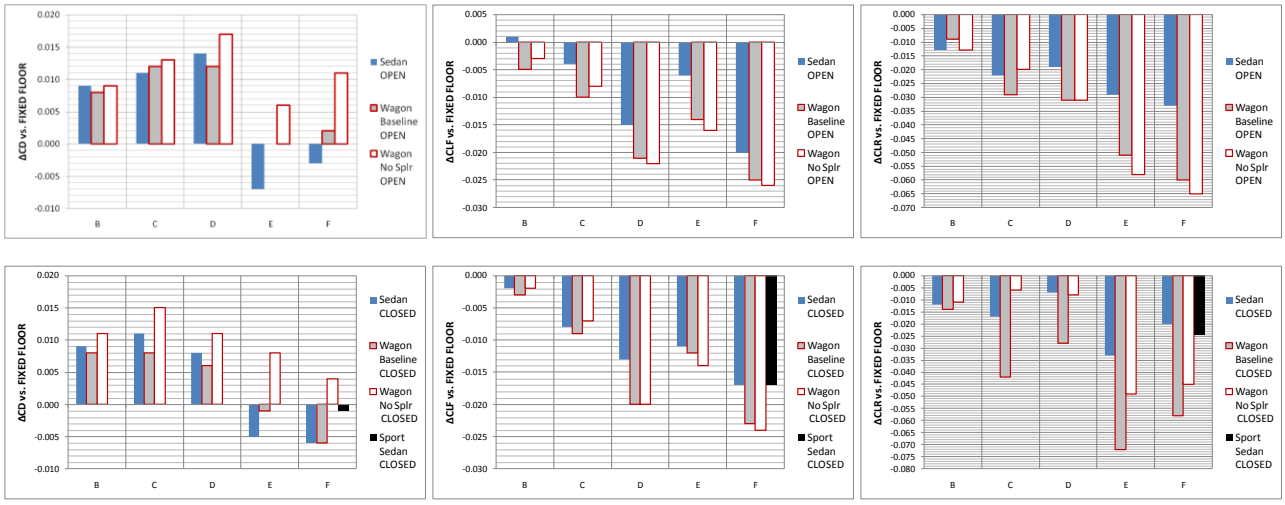

Key: Wind-Tunnel Floor Conditions

A	REF: Fixed floor mode, no boundary layer control
B	Boundary layer suction (BLS) only
C	BLS and center belt
D	BLS, belt, rotate front wheels only
E	BLS, belt, rotate rear wheels only
F	Moving ground mode (BLS, belt, rotate wheels)

Figure 4. Effect of wind-tunnel floor conditions across vehicles

Sedan Data, Simulation	Cooling			No Cooling		
	CD	CLF	CLR	CD	CLF	CLR
Fixed floor mode, no boundary layer control	0.282	0.159	0.108	0.275	0.084	0.142
Boundary layer suction (BLS) only	--	--	--	0.286	0.083	0.127
BLS and center belt	--	--	--	0.284	0.078	0.126
Moving ground mode (BLS, belt, rotate wheels)	0.279	0.152	0.090	0.277	0.077	0.119
*On-road setup (moving ground, rotate wheels)	--	--	--	0.272	0.075	0.119

Wagon Baseline with Underbody Spoiler, Simulation	Cooling			No Cooling		
	CD	CLF	CLR	CD	CLF	CLR
Fixed floor mode, no boundary layer control	0.306	0.123	0.108	0.311	0.051	0.137
Boundary layer suction (BLS) only	0.311	0.127	0.098	--	--	--
BLS and center belt	--	--	--	--	--	--
Moving ground mode (BLS, belt, rotate wheels)	0.302	0.114	0.048	0.308	0.042	0.088

Wagon with No Underbody Spoiler, Simulation	Cooling			No Cooling		
	CD	CLF	CLR	CD	CLF	CLR
Fixed floor mode, no boundary layer control	--	--	--	0.293	0.032	0.043
Moving ground mode (BLS, belt, rotate wheels)	--	--	--	--	--	--

Sport Sedan Data, Simulation	Cooling			No Cooling		
	CD	CLF	CLR	CD	CLF	CLR
Fixed floor mode, no boundary layer control	--	--	--	0.293	0.002	0.121
Moving ground mode (BLS, belt, rotate wheels)	--	--	--	0.297	-0.001	0.082

*On-road setup was tested in simulation only, for comparison with Moving ground mode.

Table 6. Summary of simulation data for each vehicle with different wind-tunnel floor conditions.

Lattice Boltzmann Simulation Results

Effect of Vehicle Configuration. The force values computed for 14 simulation data points are shown in Table 6. An additional point labeled "On-road setup" is included for the sedan with no cooling, for comparison of fully-moving ground simulation with the moving ground wind-tunnel floor mode. Configurations were selected to test a range of effects shown in the experiment, including taped cooling apertures, wind-tunnel floor mode and removing the underbody spoiler for the wagon. The correlation with experiment shows good general agreement for drag, front lift and rear lift. The correlation for front and rear lift is presented in Figure 5 as a scatter plot for all 14 configurations: simulation values of CLF and CLR are shown on the vertical axis compared to wind-tunnel values on the horizontal axis. The vertical distance from each point to the black diagonal line shows the error relative to experiment. The trend shows front and rear lift predictions scattered around the perfect correlation line, with some points trending toward higher lift values in the simulation. Differences in the lift values between the simulation and experiment show that some further improvements are needed in matching the exact conditions of the experiment such as the effect of interference from the wind-tunnel nozzle and collector. Lift values are known to vary significantly across wind-tunnels due to these effects, and since these effects are neglected the correlation to experiment is within the expected range of uncertainty.

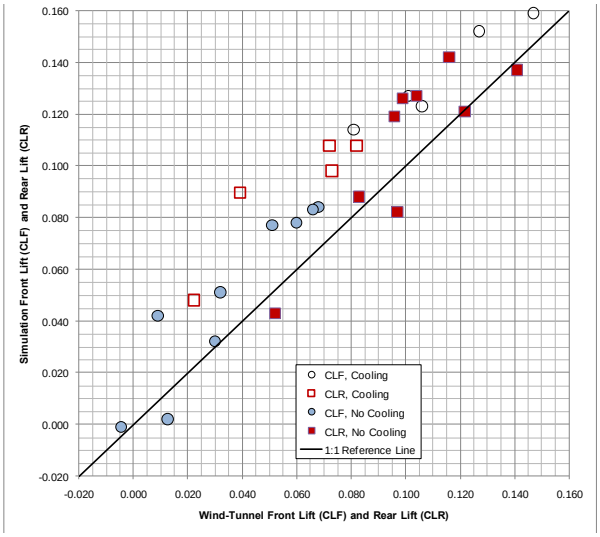

Figure 5. Summary of front and rear lift correlation between simulation and experiment, for the tests shown in Table 6.

In comparing the predicted trends, the lift deltas are also in good general agreement with experiment. The lift trends are shown as bar graphs in Figures 6 and 7. In Figure 6, the trend for closing cooling apertures is shown and matches very closely to experiment. Similarly, the spoiler effect on lift change is shown. The front lift reduction trend is over-predicted, and the large rear lift reduction in the experiment is matched in the simulation.

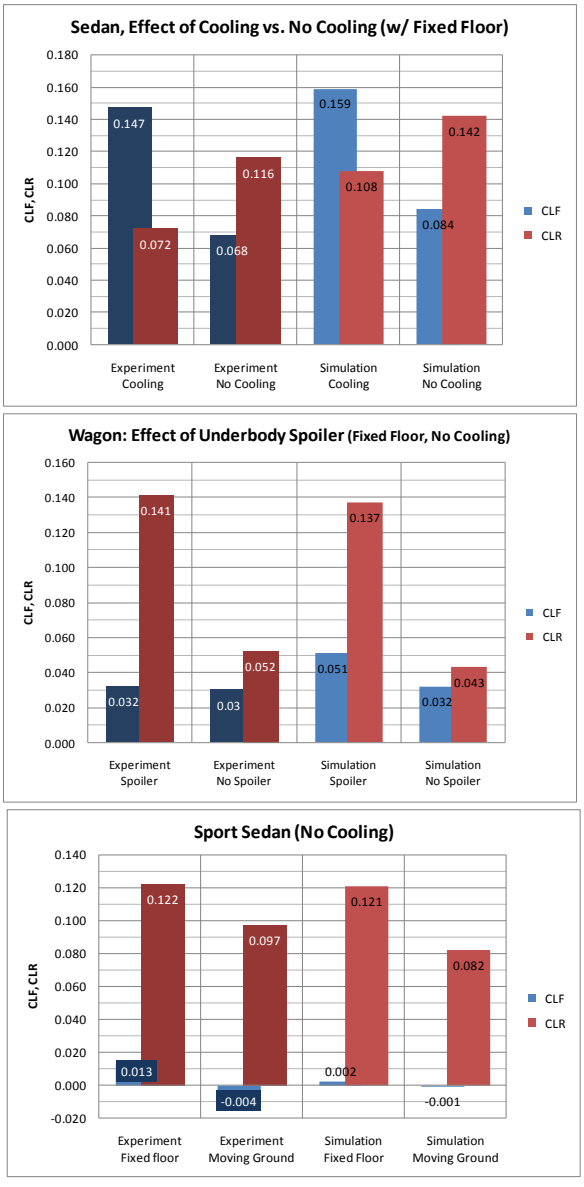

Figure 6. a) Effect of cooling vs. no cooling on front lift (CLF) and rear lift (CLR) for sedan with fixed floor, b) effect of removing underbody spoiler on front lift (CLF) and rear lift (CLR) for wagon with fixed floor, and c) effect of wind-tunnel floor mode on front lift (CLF) and rear lift (CLR) for sport sedan (no cooling).

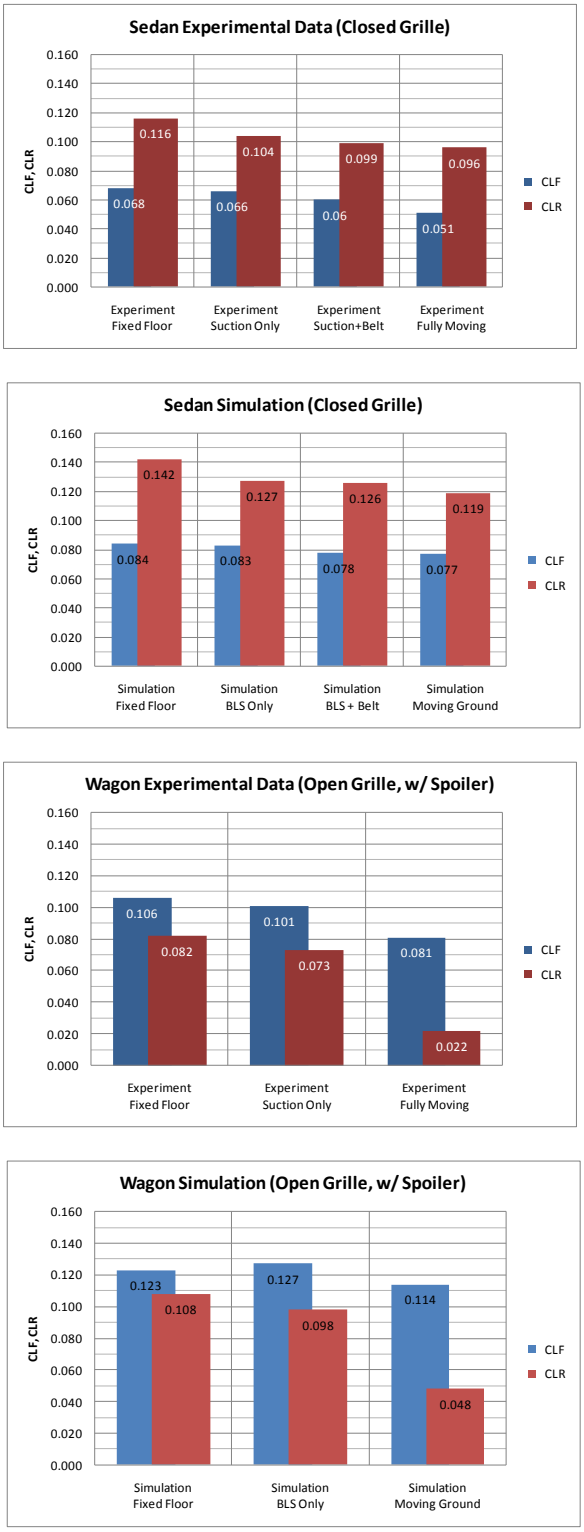

Figure 7. Effect of wind-tunnel floor mode on front lift (CLF) and rear lift (CLR) for sedan (no cooling) and wagon (with cooling).

Flow visualization images for the sedan are included in Figures 8 and 9 using the time-averaged flow field. Figure 8 shows the complex flow structure on the C-pillars, back glass and deck lid, with the static surface pressure. The lift is strongly affected by the increase of pressure at the base of the back glass as the flow coming down the glass is turned to flow horizontally into the top of the vehicle wake. As shown in Figure 9, the low pressure levels at the front of the underbody floor reduce the front lift especially with no cooling. The shape of the chin and tire deflectors causes some local high pressure regions which increase the front lift. The effect of closed cooling on the front lift can be seen as a reduction in the engine bay pressure as well as pressure under the chin area.

Figure 10 shows the effect of the underbody spoiler for the wagon. Removing the spoiler reduces the pressure under the spare tire cover. With the spoiler, the pressure increases locally on the underbody in front of the spoiler, and the flow behind the spoiler is deflected downward, with a significant impact on the bottom of the vehicle wake. The larger wake is more neutrally balanced and produces a slightly positive rear lift (CLR=0.022 in the experiment, CLR=0.048 in the simulation).

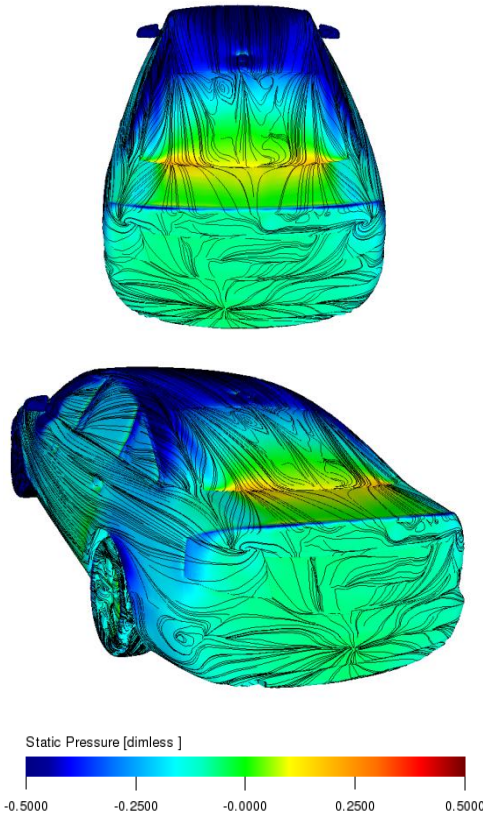

Figure 8. Surface pressure and flow pattern on rear of vehicle for sedan with no cooling and fixed floor

a) cooling, fixed floor

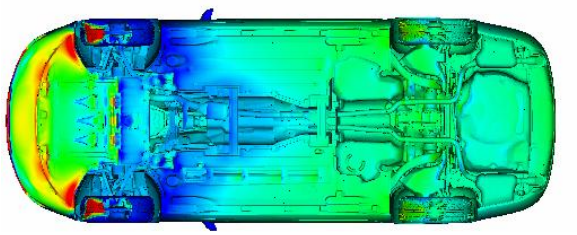

b) cooling, moving ground

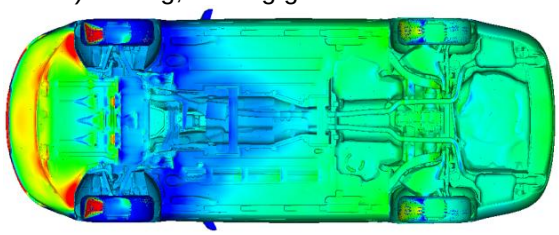

c) no cooling, fixed floor

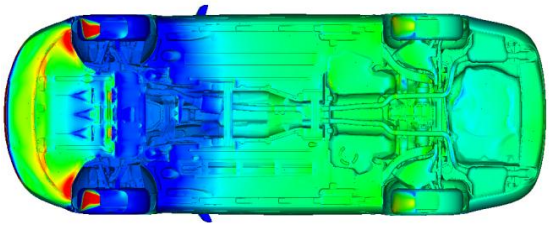

d) no cooling, moving ground

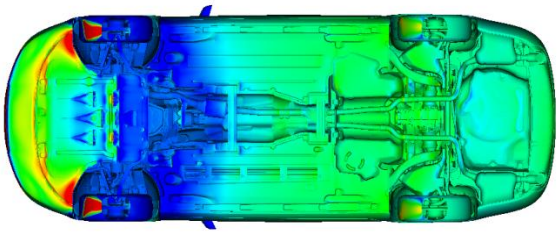

Figure 9. Surface pressure for sedan, comparing fixed floor and moving ground mode, for simulations with cooling and no cooling. Pressure caption is same as Figure 8

Effect of Wind-Tunnel Floor Mode. Figures 9 and 11 show the moving ground effect for the sedan. The pressure differences are subtle but can be seen as a distributed reduction in underbody pressure due to the moving ground, and an increase on flow speed under the center of the vehicle by the motion of the belt and wheels. The effect is shown quantitatively using integration of the drag and lift force in Figure 12. The difference in overall force for different test modes is integrated from the front to the rear of the vehicle. The effect on drag is shown comparing both the "BLS + Center Belt" and "Moving Ground" modes relative to the "Fixed Ground" mode. The boundary layer suction increases the drag on the nose

of the vehicle up to an increment of ΔCD=+0.006 in the "BLS + Center Belt" mode, and then increases further up to ΔCD=+0.008 under the vehicle at approximately X=-1.0 m (beginning of vehicle floor). The increase in drag is seen in analysis of the results to occur due to lower pressure on the front of the hood and higher pressure under the chin, so the drag increase also produces a small front lift increase.

Behind X=-1.0 m the "BLS + Center Belt" mode has neutral drag effect relative to fixed floor. The moving ground mode also shows the increase in drag due to boundary layer suction but the wheel rotation effect reduces the drag increment slightly to ΔCD=+0.006 under the vehicle. The drag increment decreases further at the very back of the vehicle which indicates that the moving ground affects the wake to increase the base pressure (which reduces drag).

a) with spoiler, no cooling, fixed ground

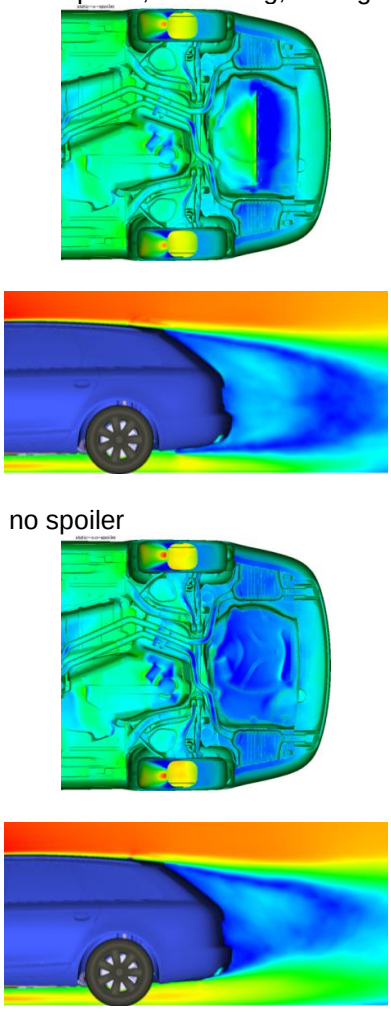

b) no spoiler

Figure 10. Surface pressure, and velocity on centerplane for wagon with no cooling and fixed ground, comparing spoiler with no spoiler

Figure 11 shows the modification in underbody flow structure caused by the moving ground conditions. The front wheel wakes are reduced, and flow is accelerated under the center of the vehicle.

The effects on incremental lift are shown in Figure 12. The boundary layer suction and center belt increase the lift by about ΔCL=+0.005 due to the pressure changes on the nose, and then decreases steadily under the vehicle floor due to a lower pressure and higher speed flow under the car. The effect of wheel rotation is to further lower the underbody pressure and bring down the lift increment.

a) fixed floor, no cooling

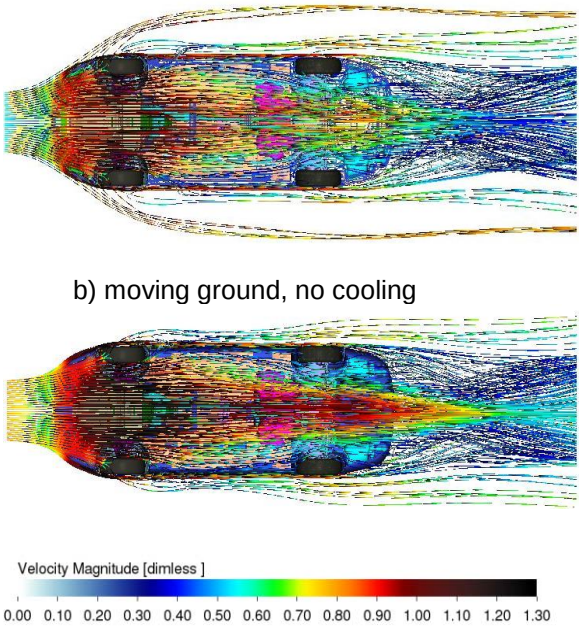

Figure 11. Streamlines in the fluid emitted in front of the nose of the vehicle, comparing fixed floor to moving ground configuration. The streamlines are colored by velocity and show the higher speed flow under the vehicle for the moving ground configuration.

Effect of On-Road vs. Moving Ground Mode.

The effect of the wind-tunnel moving system can be differentiated from the true on-road effect using simulation. For the sedan case tested, the results show that the wind-tunnel produces some drag effect that is not present on the road. In Figure 12, this is seen as the thick solid and dashed curves: the curve for "On-Road" simulation shows a neutral drag effect on the front half of the vehicle, indicating that boundary layer suction artificially increases the vehicle drag. Behind X=-1.0 m the drag difference relative to fixed ground is the same for both curves, indicating that the moving ground mode includes the same drag effects of the moving ground and

wheel rotation observed on the road on the central and rear portions of the vehicle.

Figure 12 also shows the lift difference for moving ground mode compared to "On-Road" configuration. The lift trends match closely for this vehicle, indicating that the effects of boundary layer suction, moving belt and wheel rotation on the underbody pressure distribution are similar to the effects on the road.

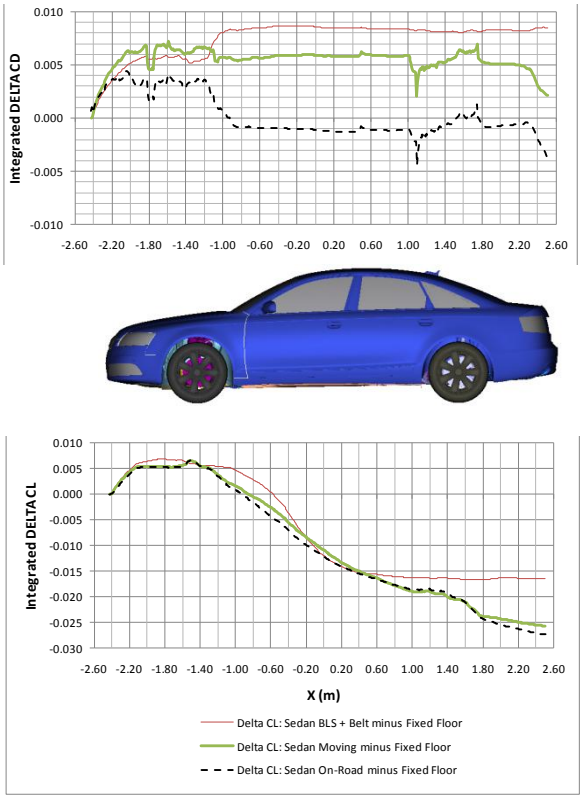

Figure 12. Integration of delta drag and delta lift distribution, for each configuration relative to Fixed Floor. The drag and lift are integrated in X from the nose to the tail of the vehicle. The integration curves are subtracted to isolate the effects of wind-tunnel floor configuration mode on the drag distribution. Comparison of the On-Road configuration to the Moving Floor configuration shows that compared to fully-moving road, the wind-tunnel moving ground system increases the drag on the front half of the vehicle.

CONCLUSIONS

This study shows how simulation can be used to predict lift effects across vehicles and configurations. Predictions show good prediction of absolute values of front and rear lift within a reasonable range of uncertainty similar to testing in multiple wind-tunnels. Trends for moving ground effects, closed cooling, and underbody spoiler were very well predicted. The results also showed that the boundary layer suction system adds drag that is not occurring in the on-road simulation with fully moving ground, but that otherwise the effects of the on-road simulation are very similar to the simulation of the moving-ground wind-tunnel.

REFERENCES

1. Wickern, H., and Lindener, N. "The Audi Aeroacoustic Wind Tunnel: Final Design and First Operational Experience", SAE Paper 2000-01-0868, 2000.
2. Wiedemann, J. and Potthoff, J.: The New 5-Belt Road Simulation System of the IVK Wind Tunnels, SAE Paper, 2003-01-0429, Detroit, 2003 .
3. Wickern, G., Wagner, A., and Zoerner, C., "Induced Drag of Ground Vehicles and Its Interaction with Ground Simulations", SAE Paper 2005-01-0872, 2005.
4. Lounsberry, T.H., Gleason, M.E., Kandasamy, S., Sbeih, K., Mann, R., Duncan, B.D., "The Effects of Detailed Tire Geometry on Automobile Aerodynamics – a CFD Correlation Study in Static Conditions", SAE Paper 2009-01-0777, 2009.
5. Duncan, B.D., and Golsch, K., "Characterization of Separated Turbulent Flow Regions in CFD Results for a Pontiac NASCAR Race Car", SAE Paper 2004-01-3556, 2004.
6. Duncan, B., Senthooran, S., Hendria, D., Sivakumar, P., Freed, D., Gleason, M., and Hall, D., "Multi-Disciplinary Aerodynamics Analysis for Production Vehicles: Application of External Flow Simulations to Aerodynamics, Aeroacoustics and Thermal Management of a Pickup Truck", SAE Paper 2007-01-0100.
7. Albukrek, C., Doddegowda, P., Ivaldi, A., and Amodeo, J., "Unsteady Flow Analysis of a Formula Type Open Wheel Race Car in Cornering", SAE Paper 2006-01-3661, 2006.
8. Senthooran, S., Crouse, B., Freed, D., Balasubramamian, G., Noelting, S., Duncan, B. and Powell, R., "Prediction of Wall Pressure Fluctuations on an Automobile Side-glass using a Lattice-Boltzmann Method", AIAA 2006-2559.

9. Lietz, R., Mallick, S., Kandasamy, S., and Chen, H. "Exterior Airflow Simulations Using a Lattice Boltzmann Approach", SAE Paper 2002-01-0596.

10. Furukawa, N., Shiozawa, H., Koyama, R., Ishihara, Y. and Aoki, H., "Application of CFD Aerodynamic Computation Methods to New Vehicle Development Based on a Model that Reproduces a 230 Engine Bay and Floor", JSAE Paper #20045513, 2004.

11. Amodeo, J., Alajbegovic. A., and Jansen, W., "Thermal Management Simulation for Passenger Cars toward Total Vehicle Analysis," 6th MIRA International Vehicle Aerodynamics Conference, Birmingham, UK, October 24-26, 2006..

12. Alajbegovic, A., Sengupta, R., and Jansen, W., "Cooling Airflow Simulation for Passenger Cars using Detailed Geometry," SAE 2006-01-3478.

13. Duncan, B.D., Sengupta, R., Mallick, S. and Sims-Williams, D.B., "Numerical Simulation And Spectral Analysis Of Pressure Fluctuations In Vehicle Aerodynamic Noise Generation", SAE Paper 2002-01-0597, 2002.

14. Crouse, B., Senthooran, S., Freed, D., Balasubramanian, G., Gleason, M., Puskarz, M., Lew, P. and Mongeau, L., "Experimental and Numerical Investigation of a Flow-Induced Cavity Resonance with Application to Automobile Buffeting", AIAA 2006-2494.